Research paper

Electrophysiological scarring in remitted depressed patients: Elevated EEG functional connectivity between the posterior cingulate cortex and the subgenual prefrontal cortex as a neural marker for rumination

Lars Benschop [a,*], Tasha Poppa [a], Takfarinas Medani [b], Hossein Shahabi [b], Chris Baeken [a,c,d], Richard M. Leahy [b], Diego A. Pizzagalli [e,1], Marie-Anne Vanderhasselt [a,1]

[a] Ghent University, Department of Psychiatry and Medical Psychology, Corneel Heymanslaan 10, 9000 Ghent Belgium
[b] University of Southern California
[c] Free University of Brussels
[d] Eindhoven University of Technology
[e] Harvard University

ABSTRACT

Introduction: Prior resting state fMRI studies have revealed that elevated connectivity between the default mode network (DMN) and subgenual prefrontal cortex (sgPFC) connectivity may underly maladaptive rumination, which is a major risk factor for depression. To further evaluate such relationship, we investigated whether posterior regions of the DMN, showed elevated connectivity with the sgPFC in remitted depressed patients (rMDD) and whether this connectivity was related to maladaptive rumination.
Methods: We examined whether rMDD ($N = 20$) had elevated EEG posterior DMN – sgPFC functional connectivity when compared to age and sex matched healthy controls ($N = 17$), and whether this posterior DMN – sgPFC connectivity positively correlated with rumination. Using minimum norm as the source estimation method, we extracted current density maps from six regions of interest (ROIs) within the posterior DMN. EEG source-space functional connectivity was calculated using the Amplitude Envelope Correlation method.
Results: Relative to controls, rMDD showed increased posterior cingulate cortex (PCC) – sgPFC connectivity in the beta-3 (25–30 Hz) band. As hypothesized, PCC – sgPFC connectivity was positively associated with rumination for rMDD, even after controlling for depression and anxiety.
Limitations: The absence of an MDD patient group and the relatively small sample size can limit the generalizability of the results.
Conclusions: EEG resting state PCC – sgPFC functional connectivity is significantly elevated in rMDD and is associated with rumination, suggesting that EEG PCC – sgPFC connectivity may be useful as a neural marker to identify individuals at risk for depression.

Introduction

Major Depressive Disorder (MDD) is one of the most prevalent psychiatric disorders worldwide (World Health Organization, 2017) and is often characterized by impaired mood, inability to experience pleasure, reduced motivation and, in severe cases, suicide. The lifetime prevalence of MDD is estimated at 20% and 30% for men and women, respectively (Kruijshaar et al., 2005). Furthermore, MDD is a leading cause of disability (Friedrich, 2017), resulting in a significant economic and societal burden through increased absenteeism, alcohol and drug-related issues, and somatic and mental comorbidity. In addition, recurrence is a major problem, as one-in-three MDD patients will develop a subsequent depressive episode (Eaton et al., 2008). Therefore, it is imperative to identify risk factors that increase the vulnerability of relapse in remitted MDD populations.

Rumination is a leading cognitive risk factor which predicts the onset, duration and recurrence of depression (Nolen-Hoeksema et al., 2008). Ruminative thinking entails repetitive and passive thoughts

---

* Corresponding author.
  E-mail address: lars.benschop@ugent.be (L. Benschop).
[1] These authors share senior authorship.

about one's negative feelings, causes and consequences (Nolen-Hoeksema and Morrow, 1991). It is a maladaptive coping strategy in response to stressful life events, in which the individual remains fixated on the problems he or she experiences and the negative feelings they bring about, yet without engaging in active problem solving. Rumination has a robust association with MDD that persists even after controlling for other maladaptive cognitive styles such as perfectionism, neuroticism and pessimism (Flett et al., 2002; Nolen-Hoeksema et al., 1994; Spasojević and Alloy, 2001). Moreover, rumination has been found to significantly mediate the relationship between depression and dysfunctional attitudes, self-criticism, negative inferential styles and neuroticism (Ito et al., 2005; Nolan et al., 1998; Nolen-Hoeksema et al., 1994; Spasojević and Alloy, 2001). Altogether, the evidence indicates that rumination is a crucial mechanism underlying MDD (Flett et al., 2002; Nolen-Hoeksema et al., 1994, 2008; Spasojević and Alloy, 2001).

Within the past two decades, advancements in neuroscience have elucidated the neurobiological underpinnings of MDD. Neuroimaging research has shifted from focusing on individual brain regions affected in MDD to understanding the symptomatology through abnormalities within-and-between brain networks. A brain network model for depression recently proposed by Li and colleagues (Li et al., 2018) conceptualized MDD symptomatology in terms of dysregulation within four intrinsic functional brain networks, including the default mode network (DMN), which comprises the precuneus, posterior cingulate cortex (PCC), the angular gyrus and the medial prefrontal cortex (mPFC) (Andrews-Hanna et al., 2010). DMN activity is associated with passive, internally directed mental states such as self-referential processing, autobiographical memory retrieval, and imagining future events (Buckner et al., 2008; Gusnard et al., 2001; Raichle et al., 2001). In contrast, focusing on external events or engaging in goal-directed behaviors activates the fronto-parietal cognitive control network, which inhibits DMN activity if it is irrelevant to task performance (Chen et al., 2013).

In the past decade, resting state functional magnetic resonance imaging (fMRI) studies have reported hyper-connectivity of the DMN in patients suffering from MDD (Berman et al., 2011; Greicius et al., 2007; Hamilton et al., 2011b; Ho et al., 2015; Sheline et al., 2010; Zhu et al., 2012). Enhanced DMN connectivity seems to be an enduring marker of depression that can be observed in adults (Berman et al., 2011; Greicius et al., 2007; Hamilton et al., 2011b; Sheline et al., 2010; Zhu et al., 2012), adolescents (Ho et al., 2015), and children (Gaffrey et al., 2012). Considering the involvement of the DMN with self-referential processing (Gusnard et al., 2001), elevated DMN activity observed in MDD could be interpreted as relating to the disproportionate negative self-focus and maladaptive rumination that characterizes this disorder (Berman et al., 2014, 2011; Li et al., 2018; Zhu et al., 2012). Indeed, enhanced DMN connectivity has been found to be associated with depressive rumination in individuals with current MDD (Berman et al., 2014, 2011; Zhu et al., 2012), past MDD (Nixon et al., 2014; Zamoscik et al., 2014) and even in healthy subjects (Berman et al., 2014, 2011). Additionally, one study reported increased DMN connectivity in MDD patients after rumination was induced as compared to an uninstructed resting state (Berman et al., 2014). Such results emphasize the importance of ruminative states on elevated DMN connectivity.

Expanding on the findings of the association between increased DMN connectivity and rumination, Hamilton and colleagues (Hamilton et al., 2015) proposed that the relationship between maladaptive rumination and DMN hyper-connectivity is actually driven by enhanced connectivity between the DMN and the subgenual prefrontal cortex (sgPFC). These researchers argue that while the DMN is involved with self-referential processing (Gusnard et al., 2001), the sgPFC is associated with negative affective processing (Etkin et al., 2011). Therefore, hyper-connectivity of the DMN with the affect-laden sgPFC results in a state of excessive negative self-focus, which is the central aspect of maladaptive rumination (Hamilton et al., 2015). This view is supported by a number of studies which showed how elevated connectivity

between the sgPFC and DMN predicted rumination intensity in depression (Berman et al., 2011; Hamilton et al., 2011a; Zhu et al., 2012).

Although fMRI is an essential tool to uncover neurobiological mechanisms behind MDD, the clinical feasibility of using fMRI-derived biomarkers is limited since fMRI is expensive, time consuming, or frequently unavailable. In contrast, the electroencephalogram (EEG) is a cost-effective, time-efficient and widely available neuroimaging tool that has been routinely applied for diagnostics of neuropsychiatric disorders and epilepsy (Ney et al., 2013; Olbrich and Arns, 2013). In addition, EEG's superior temporal resolution allows us to examine functional connectivity of neural oscillations across a broad frequency range, whereas fMRI connectivity is limited by the relatively slow hemodynamic response, constraining the frequency range up to 1 Hz. Therefore, EEG functional connectivity can be utilized to investigate whether brain networks have unique electrophysiological frequency signatures. Evidence has indicated that the beta band is involved with DMN connectivity, since multiple combined fMRI/EEG connectivity studies found a significant positive association between fMRI DMN connectivity and EEG beta band power (Hlinka et al., 2010; Mantini et al., 2007; Neuner et al., 2014), suggesting that the beta band is a frequency range of importance for DMN connectivity.

Until recently, estimating EEG functional connectivity was problematic due to the inherent diffusion of electrical signals caused by volume conduction of the skull and the surrounding soft tissues. Advances in EEG source localization such as the development of high density EEG (whole-head electrode coverage) (Song et al., 2015), realistic head models (Gramfort et al., 2010; Vorwerk et al., 2014) and more reliable linear inverse solutions (Baillet et al., 2001) have made it possible to significantly reduce the spatial inaccuracies of electromagnetic signals (Michel and He, 2012). Furthermore, many measures of stationary or resting state connectivity exist for EEG, such as imaginary coherence, phase-locking value, phase lag index and amplitude envelope correlation (AEC). A recent study from Colclough and colleagues (Colclough et al., 2016) compared 12 functional connectivity measures to estimate brain networks with electromagnetic signals and found that AEC and partial correlation measures have the most intra-subject and between group consistency. Their findings demonstrate that by applying orthogonalization correction to AEC, spatial leakage artefacts are minimized, which are a major source of spurious connectivity in electromagnetic signals. Conversely, phase- and coherence-based measures of connectivity such as imaginary coherence and phase lag index performed poorly despite being widely used as functional connectivity metrics in EEG research.

While some EEG studies have examined abnormal network connectivity in MDD populations (Olbrich et al., 2014; Whitton et al., 2018), none have explored the relationship between enhanced DMN – sgPFC connectivity and rumination. Since rumination is a crucial risk factor for the onset and recurrence of a depressive episode, it is imperative to investigate whether DMN – sgPFC hyper-connectivity is present within the EEG resting state of a population at risk for depression, and whether this connectivity is associated with higher maladaptive rumination. Given the high rates of relapse in remitted (rMDD) patients and the importance of maladaptive rumination in MDD recurrence, we hypothesized that rMDD patients would demonstrate increased DMN – sgPFC connectivity during the EEG resting state when compared to healthy controls. In addition, we hypothesized that enhanced DMN – sgPFC connectivity would be positively associated with maladaptive rumination, which may indicate that the EEG resting state could be a potential biomarker for individuals at risk for depression.

Methods

Participants

The study sample was comprised of 37 participants recruited from the Greater Boston area and was recruited from the Laboratory of

Affective Neuroscience at Harvard University for an event-related potentials study (Vanderhasselt et al., 2012). The internet was used to invite individuals for an initial phone screening. Eligible participants were invited for a Structured Clinical Interview for DSM-IV (SCID) (First et al., 2002). The SCID was administered by a Master's-level, licensed mental health counsellor. Exclusion criteria for all participants included a history of neurological conditions such as loss of consciousness for more than 5 min, substance abuse during the year before data collection, current use of psychotropic medication and current psychopathology. Healthy controls were required to have no current Axis I diagnoses, and no family history of past mood disorders. RMDD patients were required to have no current Axis I diagnoses or past mood disorders other than MDD. Moreover, the criteria for rMDD patients included remission from at least 1 MDD episode in the last 5 years, remission for at least 6 months before data collection (Blackburn et al., 1986), no usage of psychotropic medications for at least 16 weeks before data collection (Kato et al., 2020). This resulted in 20 rMDD patients and 17 healthy controls.

Prior to EEG assessment, participants completed the Beck Depression Inventory II (BDI-II) (Beck et al., 1996), Rumination Response Scale (RRS) (Treynor et al., 2003) and the Mood and Anxiety Symptom Questionnaire (MASQ) (Watson et al., 1995). The RRS is a widely used questionnaire to measure ruminative tendencies. The RRS consist of three distinct factors: RRS reflection, RRS brooding and RRS depression. RRS brooding is considered to measure passive and maladaptive ruminative thought, while RRS reflection measures an active and adaptive form of rumination. RRS depression is a subscale of the RRS that measures aspects of rumination that are highly confounded with depression symptoms. All participants signed an informed consent and agreed upon the data being used for research purposes. For a more detailed description of participant recruitment we refer to the original study of Vanderhasselt and colleagues (Vanderhasselt et al., 2012).

EEG procedure and preprocessing

The EEG resting state data were acquired with a 128-channel Geodesic Sensor Net System (Electrical Geodesic, Inc., Eugene, OR [EGI]) within an electrically and acoustically shielded room. The EEG signals were sampled at 250 Hz while an analogue filter was used with a bandwidth of 0.01 Hz – 100 Hz. Electrode impedances were < 45 kΩ while the data were referenced online to the Cz. The resting state was collected in eight 1-minute segments (four minutes of eyes open and four minutes of eyes closed, counterbalanced across subjects). Due to the possible confounding effect of visual scenes on the resting state (Fingelkurts and Fingelkurts, 2015), only the eyes-closed data were included in the analysis.

A semi-automated EEG preprocessing pipeline was applied in MATLAB (Version R2019b, The MathWorks, Inc., Natick, MA) using functions from the EEGLAB toolbox (Delorme and Makeig, 2004) and the Signal Processing toolbox. The data were filtered offline with a 1 Hz high-pass and a 60 Hz low-pass filter. Signal noise was removed with the *cleanline* function which employs a statistical threshold method to subtract estimated line noise from the time series data (Bigdely-Shamlo et al., 2015). The detection of bad/noisy channels was done with the *clean_rawdata* function using the following three criteria: a) channel flatline lasting longer than five seconds, b) channel noise exceeding four standard deviations relative to its own signal and c) the correlation of a channel lower than 0.85 with its neighboring channels. Artefacts were removed from the resting state data using the Artifact Subspace Reconstruction (ASR) method. ASR is a validated artefact removal method (Chang et al., 2020) that decomposes the channel time series data into principal components. Artifactual components are detected by comparing the components against components from the data's cleanest segments. These artefactual components are removed, and the remaining components are then used to reconstruct the data without the original artefacts. The EEG data were re-referenced to the average prior to Independent Component Analysis (ICA) (Makeig et al., 1995) while

taking the adjusted data rank into account. Remaining muscle, electrocardiogram, and eyeblink artefacts were manually removed using ICA. Rejected channels were interpolated using the spline interpolation method (Perrin et al., 1987). As a final preprocessing step, both the EEG frequency power spectrum and the time series data were visually inspected.

Preliminary analysis

A preliminary analysis was conducted in R (version 4.0) on participants' demographic and clinical characteristics. Chi-square and student t-tests were performed to determine whether groups differed on age, gender, education level, ethnicity, BDI, RRS, and MASQ scores.

EEG source-space functional connectivity analysis

The EEG source-space functional connectivity analysis was computed using the MATLAB toolbox Brainstorm (Tadel et al., 2011). The USCBrain atlas (Joshi et al., 2017) was chosen as the common brain anatomy template for every participant. The USCBrain anatomy template (http://brainsuite.org/uscbrain-description/) is a high-resolution single-subject atlas that was created using both anatomical and functional data for cortex parcellation. The functional sub-parcellation was achieved by using human connectome fMRI data (Glasser et al., 2013) from 40 subjects, resulting in 65 regions of interest (ROIs) per hemisphere. EEG electrode co-registration was accomplished by using landmarks (Nz, Iz, Cz, RPA and LPA) to convert arbitrary X, Y and Z coordinates to Montreal Neurological Institute (MNI) coordinates. Furthermore, a realistic head model was computed by applying the Boundary Element Method on the USCBrain anatomy template using openMEEG (Gramfort et al., 2010). Therefore, the generated realistic head model was identical for each subject. To estimate sensor noise for the source localization model, a noise covariance matrix was calculated on the resting state data for each participant, while retaining only the diagonal elements of the matrix. Minimum norm imaging (Baillet et al., 2001) was used as a source estimation method to generate current density maps with unconstrained dipole orientations for each participant.

Based on the brain network model for depression (Li et al., 2018), six ROIs of the USCBrain atlas were selected for the source-space functional connectivity analysis: the angular gyrus, the PCC and the sgPFC for both hemispheres (Fig. 1). The precuneus and mPFC were not included in the DMN – sgPFC analysis for several reasons. First, due to the proximity of the precuneus with the PCC and the sgPFC with the mPFC, combined with the low spatial resolution of EEG source localization, autocorrelation between those regions would be high. Second, an fMRI study by Berman et al. (Berman et al., 2011) reported a positive correlation between PCC – sgPFC connectivity and maladaptive rumination in both depressed and healthy individuals, pointing to a specific relationship between those two regions and rumination. Third, the number of ROIs considerably affects the number of statistical tests. A large number of tests would have made the statistical thresholding overly conservative, which can lead to false negative results. Therefore, the EEG source-space functional connectivity analysis only included a limited number of DMN nodes.

DMN – sgPFC functional connectivity was computed in Brainstorm using the orthogonalized AEC method described by Brookes and colleagues (Brookes et al., 2011, 2012) (Fig. 2). In short, AEC is estimated by applying a Hilbert transform to the band-pass filtered time series data which is extracted from each ROI. This results in an analytical signal from which the magnitude is taken to calculate the power envelopes. Prior to the calculation of the power envelopes, a symmetric orthogonalization procedure is applied to remove the zero-lag signal that is shared between the ROIs, thereby correcting for spatial leakage artifacts. A linear correlation between the power envelopes of different ROIs is then calculated to estimate their connectivity, resulting in a connectivity
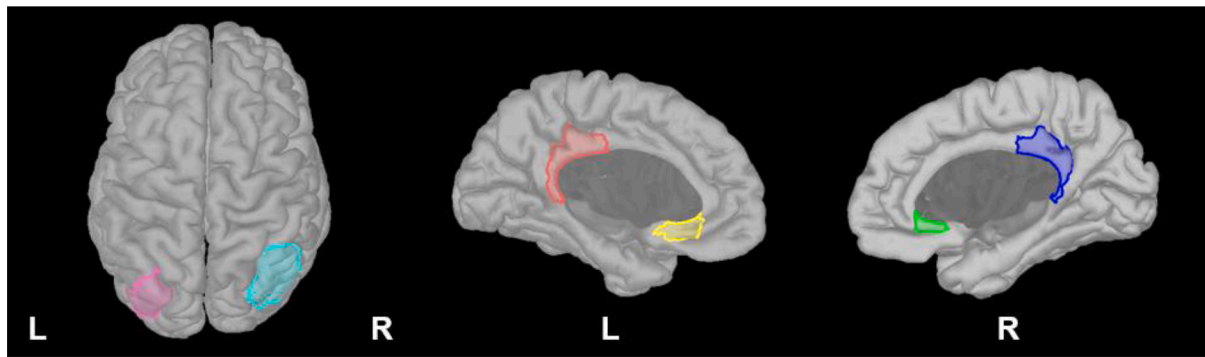
Fig. 1. The six ROIs used in the source-space connectivity analysis.
Note. The six ROIs include the left Angular Gyrus (purple), right Angular Gyrus (turquoise), left Posterior Cingulate Cortex (red), right Posterior Cingulate Cortex (blue), left subgenual Prefrontal Cortex (yellow) and the right subgenual Prefrontal Cortex (green). (For interpretation of the references to colour in this figure legend, the reader is referred to the web version of this article.)
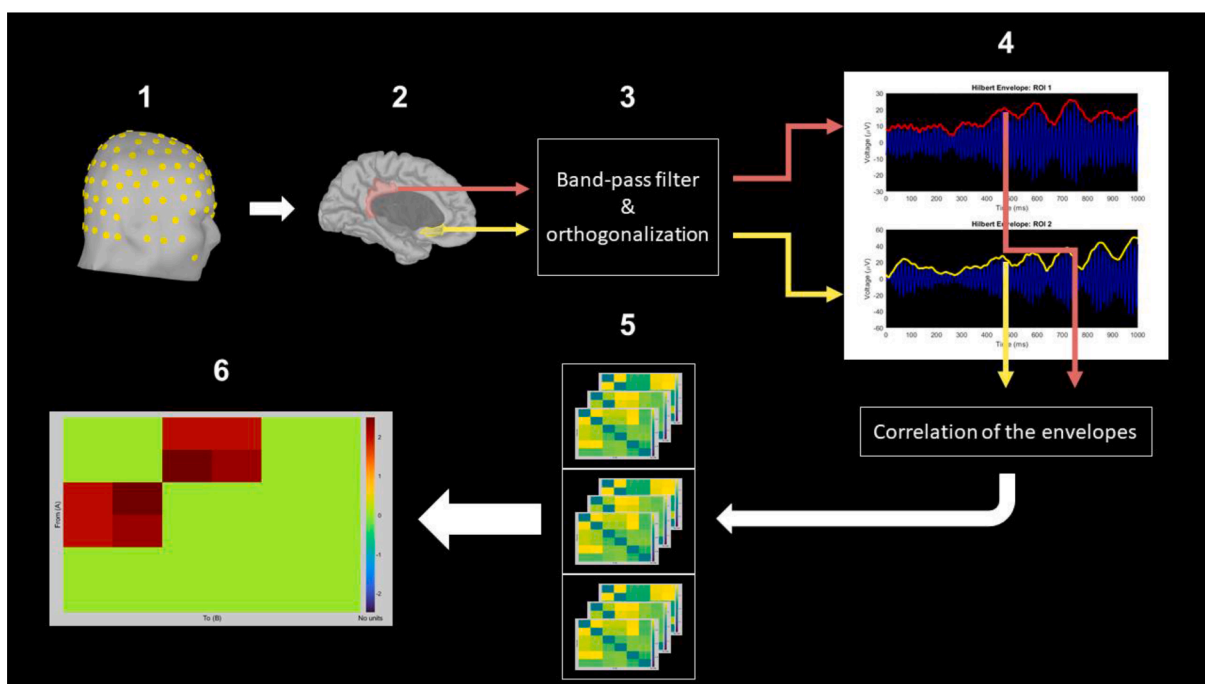

Fig. 2. EEG source-space functional connectivity using the orthogonalized Amplitude Envelope Correlation method.
Note. The computation and statistical evaluation of the orthogonalized Amplitude Envelope Correlation has been performed in six steps: The EEG resting state time series data were source localized using the minimum norm method from the sensor space (1) to the source space (2). Hypothesis driven regions of interest were defined and their time series data extracted so that band-pass filters together with an orthogonalization procedure could be applied (3). A Hilbert Transform was then used to produce the envelopes of the band-pass filtered signals so that correlations could be calculated between the signal envelopes of the different regions of interest (4). This resulted in connectivity matrices for each frequency band of interest per subject (5). Non-parametric permutation tests were then performed, resulting in statistical maps that were thresholded using the false discovery rate (6). (For interpretation of the references to colour in this figure legend, the reader is referred to the web version of this article.)

matrix for each frequency band of interest. Based on the findings of prior EEG studies (Hlinka et al., 2010; Whitton et al., 2018), the beta band seems to be predominantly involved in DMN connectivity. Therefore, the frequency bands of interest were beta-1 (13–20 Hz), beta-2 (20–25 Hz) and beta-3 (25–30 Hz).

The AEC connectivity matrices of the two groups were statistically evaluated in Brainstorm by performing non-parametric permutation *t*-tests, resulting in statistical maps for each frequency band. These statistical maps were then thresholded to correct for the number of ROI pair tests by applying the Benjamini and Hochberg's false discovery rate (FDR) method (Yekutieli and Benjamini, 1999).

Correlations between EEG source-space functional connectivity and maladaptive rumination scores

Correlations between RRS scores and extracted connectivity values were calculated in R. The correlations were calculated using Monte Carlo permutations since the connectivity values are non-normally distributed. The association between the RRS, its subscales and the connectivity values were statistically evaluated with two-tailed, FDR-corrected tests of the Pearson's correlation coefficient (*r*).

Results

Participant demographic and clinical characteristics

Demographic and clinical characteristics are summarized in Table 1. There were no significant differences between rMDD and healthy controls regarding gender, age and ethnicity. However, groups did differ significantly on education with healthy controls having on average a higher level of education than the rMDD group. Furthermore, the rMDD group scored significantly higher than the healthy controls on the BDI-II and all RRS subscales. In addition, the rMDD group scored significantly higher on the MASQ-GDA and MASQ-GDD subscales, but there were no significant group differences on the MASQ-AA and MASQ-AD subscales.

EEG source-space AEC connectivity differences between rMDD and healthy controls

The non-parametric permutation t-tests revealed significant differences ($p<0.05$, uncorrected) in AEC connectivity between rMDD and healthy controls within the beta-3 (25–30 Hz) band but not within the beta-1 (13–20 Hz) and beta-2 (20–25 Hz) band. As hypothesized, the rMDD group exhibited enhanced AEC connectivity in the beta-3 (25–30 Hz) band for the following five ROI pairs: left PCC – left sgPFC (p = 0.017), right PCC – left sgPFC (p = 0.006), left PCC – right sgPFC (p = 0.022), right PCC – right sgPFC (p = 0.010) and right sgPFC – left sgPFC (p = 0.038). A FDR threshold was applied on the ROI pair dimension to control for the number of ROI pair tests ($q<0.1$, adjusted p-value = 0.022) which yielded thresholded connectivity for the following four ROI pairs: left PCC – left sgPFC, right PCC – left sgPFC, left PCC – right sgPFC and right PCC – right sgPFC (Fig. 3).

Association between AEC connectivity values and rumination scores

To determine whether the elevated functional connectivity was associated with higher maladaptive rumination in rMDD patients, we extracted the connectivity values of the ROI pair with the strongest effect size (i.e. right PCC – left sgPFC) and correlated them with the RRS scores. The analysis revealed that PCC – sgPFC connectivity had a significant positive association with RRS sum scores within rMDD patients (r = 0.54, adjusted-p = 0.022, N = 20). Moreover, this positive
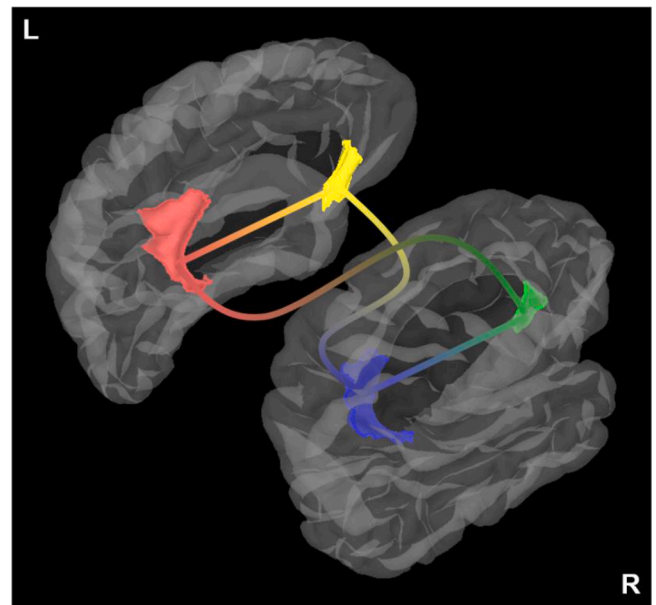

Fig. 3. Elevated remitted depressed Amplitude Envelope Correlation connectivity after FDR thresholding.
Note. Remitted depressed patients show enhanced functional connectivity in the beta-3 (25–30 Hz) band when compared to healthy controls between the following ROI pairs: left PCC (red) – left subgenual PFC (yellow), left PCC – right subgenual PFC (green), right PCC (blue) – right subgenual PFC and right PCC – left subgenual PFC. This result was obtained after FDR thresholding to control for the number of ROI pair tests. (For interpretation of the references to colour in this figure legend, the reader is referred to the web version of this article.)

association remained significant after controlling for BDI-II scores and MASQ-GDA scores (partial r = 0.49, adjusted-p = 0.037, N = 20) via partial correlation, implying that the positive association between PCC – sgPFC connectivity and rumination was not driven by depression- and anxiety scores. In addition, similar positive associations were found between PCC – sgPFC connectivity with RRS reflection (partial r = 0.6, adjusted-p = 0.022, N = 20) and RRS brooding (partial r = 0.48, adjusted-p = 0.045, N = 20) but not with RRS depression (partial r = 0.33, p = 0.104, N = 20), demonstrating that the relationship is unique to RRS items not confounded with depression. Fig. 4 shows the correlations between PCC – sgPFC connectivity values and the RRS and its subscale scores for rMDD patients. The finding that PCC – sgPFC was positively associated with both brooding and reflection is conceptually important, considering that brooding is described as a maladaptive form of rumination, while reflection is deemed an adaptive form of rumination (Joormann et al., 2006).

Discussion

In order to reduce the substantial personal, societal and economic burden associated with MDD, it is critical to identify risk factors leading to the onset and recurrence of this prevalent disorder. Prior fMRI research has highlighted the involvement of DMN hyper-connectivity in MDD (Greicius et al., 2007; Ho et al., 2015; Li et al., 2013; Sheline et al., 2010) and the association of DMN – sgPFC connectivity with maladaptive rumination (Berman et al., 2014, 2011; Zhu et al., 2012), which is a major risk factor for developing depression (Flett et al., 2002; Nolen-Hoeksema et al., 1994, 2008; Spasojević and Alloy, 2001). However, there are practical advantages of EEG for clinical assessments, as discussed in the introduction. Nevertheless, few EEG studies have examined DMN connectivity in depression (Olbrich et al., 2014; Whitton et al., 2018), and none have explored the relationship between DMN – sgPFC connectivity and rumination.
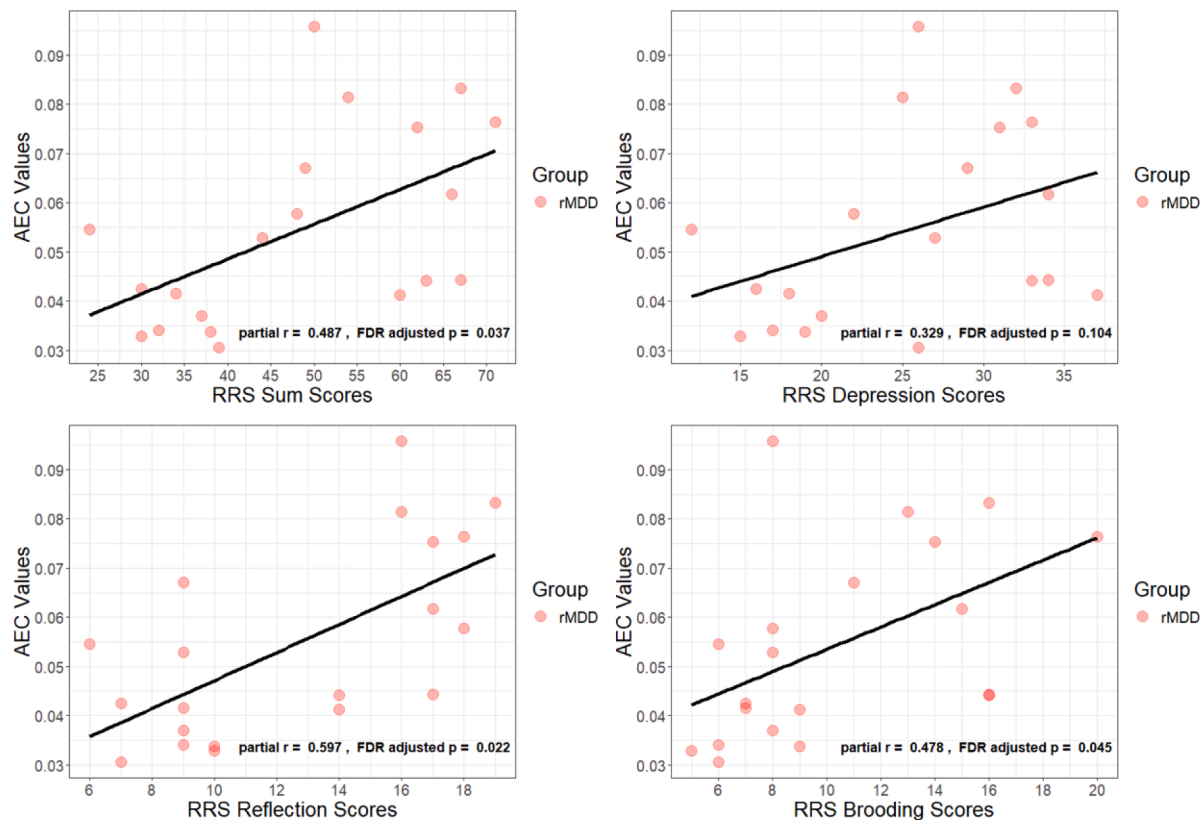
Table 1

Participant demographic and clinical characteristics. Note. Numerical data entries are in the form: mean (sd). Statistical evaluation was conducted with chi-square tests (χ^2) and student t-tests (t).

	HC ($n = 17$)	rMDD ($n = 20$)	test value	df	p value
Demographics					
Female, N (%)	9 (52.9)	9 (45)	χ^2=0.23	1	0.631
Age in years	29.4 (11.2)	27.5 (7.3)	t = 0.62	35	0.542
Education level, N (%)	L1 = 6 (35.3)	L1 = 7 (35.0)	χ^2=8.73	3	0.022
	L2 = 5 (29.4)	L2 = 13 (65.0)	–	–	–
	L3 = 4 (23.5)	L3 = 0 (0.0)	–	–	–
	L4 = 2 (11.8)	L4 = 0 (0.0)	–	–	–
Caucasian, N (%)	13 (76.5)	17 (85.0)	χ^2=2.64	4	0.766
Symptomatology					
BDI-II	1.4 (2.7)	5.3 (4.9)	t=−2.85	35	0.007
RRS D	16.0 (5.2)	25 0.3 (7.5)	t=−4.20	35	<0.001
RRS B	7.2 (2.0)	10.4 (4.4)	t=−2.52	35	0.017
RRS R	8.5 (3.5)	12.6 (4.4)	t=−2.99	35	0.005
MASQ GDA	13.7 (2.7)	15.7 (2.8)	t=−2.18	35	0.036
MASQ AA	18.4 (1.8)	19.1 (3.1)	t=−0.79	35	0.433
MASQ GDD	14.5 (2.6)	17.8 (4.4)	t=−2.67	35	0.011
MASQ AD	120.3 (9.7)	114.6 (11.6)	t = 1.60	35	0.118

Fig. 4. Scatterplots demonstrating the positive association between RRS scores and PCC – sgPFC Amplitude Envelope Correlation connectivity for remitted depressed patients.

Note. Amplitude Envelope Correlation connectivity values from the right PCC – left sgPFC were correlated with the RRS sum scores, RRS depression scores, RRS reflection scores and RRS brooding scores using non-parametric partial Pearson correlation coefficients for remitted depressed patients.

Therefore, we addressed the question of whether individuals at risk for developing depression exhibit increased connectivity between nodes of the posterior DMN and the sgPFC during resting state EEG compared to healthy controls, and whether this elevated connectivity is associated with maladaptive rumination. Our findings showed that rMDD patients were characterized by significantly enhanced connectivity between an important region of the DMN (the PCC) and the sgPFC within the beta-3 (25–30 Hz) band when compared to healthy controls. Furthermore, PCC – sgPFC connectivity was positively correlated with questionnaire scores of maladaptive rumination within rMDD patients. Critically, this correlation remained significant when controlling for measures of depression and anxiety, implying a unique relationship between PCC – sgPFC connectivity and maladaptive rumination which could be a marker for depression risk.

These results fit prior fMRI reports that have investigated the association between DMN – sgPFC connectivity and rumination (Berman et al., 2014, 2011; Zhou et al., 2020; Zhu et al., 2012). For example, a study by Berman and colleagues (Berman et al., 2011) observed a strong correlation between PCC – sgPFC resting state connectivity and RRS scores for both MDD patients and healthy controls. Furthermore, a recent meta-analysis (Zhou et al., 2020) reported that rumination associated DMN hyper-connectivity is mainly observed within the PCC and anterior prefrontal regions, suggesting that the PCC has an essential role in ruminative thought. Considering that the PCC has been implicated in autobiographical search and retrieval processing (Sestieri et al., 2011) and self-centered spatial navigation (Spreng et al., 2009), the PCC together with the ventromedial prefrontal cortex is believed to attribute valence to internalized self-centered stimuli (Northoff and Bermpohl, 2004). Based on these and other findings, Hamilton and colleagues (Hamilton et al., 2015) proposed that the self-referential processing of these core DMN regions, combined with excessive sgPFC connectivity,

results in a ruminative state that is characterized by disproportionate negative self-focus and withdrawn behaviors. This theoretical model corroborates our findings regarding PCC – sgPFC hyper-connectivity within rMDD patients and could explain why we did not observe elevated connectivity between the angular gyrus and the sgPFC.

Nevertheless, some fMRI studies of MDD patients report contrary findings which show either reduced connectivity (Anand et al., 2005; Guo et al., 2013) or simultaneously reduced- and increased connectivity (Guo et al., 2014; Zhu et al., 2012) with various DMN nodes. While the findings of these ostensibly similar studies appear to inconsistent with the findings of the current study, there are important differences that may explain the divergence. Although Anand et al. (2005) found reduced connectivity of medial prefrontal regions, they mainly reported reduced connectivity between the medial prefrontal regions with the limbic system such as the amygdala. Reduced cortico-limbic connectivity in Anand and colleagues' study was furthermore linked to emotional dysregulation. However, it should be emphasized that while emotional dysregulation is a core symptom of depression, it is distinct from maladaptive rumination. Guo and colleagues reported reduced PCC connectivity with the superior frontal gyri (Guo et al., 2013), decreased network homogeneity in the inferior temporal gyrus, and increased network homogeneity in the dorsal mPFC (Guo et al., 2014). In general, inconsistent findings among studies of DMN functional connectivity in MDD could be explained by the multifaceted function of the DMN. ICA-derived network studies have shown that the DMN could be subdivided in two subsystems: (1) an anterior DMN (aDMN) which contains the mPFC, PCC and the anterior cingulate cortex and (2) a posterior DMN (pDMN) which also contains the PCC but not the mPFC. (Damoiseaux et al., 2008; Lei et al., 2014, 2013; Xu et al., 2016). Functionally, aDMN demonstrated higher activity when self-referential processing was related to the present whereas the pDMN was more

active when self-referential processing was related to the future (Xu et al., 2016). Since rumination is defined as repetitive, negative dwelling on present feelings or past events, it is more likely to involve the aDMN than the pDMN. This aDMN/pDMN distinction could explain why some studies report reduced PCC connectivity with some DMN nodes within MDD patients. Lastly, one fMRI study did report an association between increased frontal DMN connectivity and rumination without the involvement of the PCC (Zhu et al., 2012). However, the weight of any individual study should be considered in light of a recent fMRI meta-analysis concerning the DMN and rumination in patients with MDD, which provides supporting evidence for the role of the PCC within DMN connectivity and its association with maladaptive rumination (Zhou et al., 2020).

Our findings show that EEG PCC – sgPFC functional connectivity was not only associated with maladaptive rumination such as brooding, but also with reflection, which is seen as an adaptive form of rumination. This contradictory finding may seem surprising. However, multiple studies (Lyubomirsky and Nolen-Hoeksema, 1993; Marroquín et al., 2010; Nolen-Hoeksema et al., 2008; Takano and Tanno, 2009) have provided context for understanding how adaptive and maladaptive rumination inter-relate in depression-prone and depression-resilient individuals. Marroquin and colleagues (Marroquín et al., 2010) found that the adaptive effect that is attributed to reflection was dependent on the coping style of the individual. Participants who employed passive coping strategies and who frequently engaged in reflective thoughts exhibited greater symptoms of depression. Individuals with active coping strategies, however, did not show an association between reflection and depression risk. Another study revealed that reflection significantly predicted rumination (Takano and Tanno, 2009). Specifically, individuals who frequently engage in reflection were more likely to run the risk of getting stuck in ruminative thoughts when they are no longer able to find constructive solutions for their issues, thereby negating the adaptive qualities of reflection. These findings would explain our observed correlations between PCC – sgPFC connectivity with both reflection and brooding since frequent ruminators are more prone to reflect than infrequent ruminators. This interpretation is supported by demographic and clinical characteristics of our sample, which showed that the rMDD group had significantly higher RRS brooding and RRS reflection scores than the healthy control group.

The following limitations must be kept in mind when interpreting the current results. The sample size of 37 participants is relatively small, especially when one considers the low signal-to-noise ratio of EEG. This could have affected the power of our study, which also contributed to our decision to limit the number of ROIs in the analysis. Relatedly, the inherent spatial limitations of EEG also informed our choice to omit several DMN nodes in the source-space analysis such as the precuneus and the mPFC. Furthermore, although we adopted a high density – whole head EEG montage and computed a realistic head model based on a high-resolution anatomical atlas, we did not acquire structural MRI scans from our participants, which reduces the spatial accuracy of the EEG source localization. Therefore, the ROI functional connectivity values could represent activity from neighboring brain regions. Lastly, the absence of an MDD patient group limited the generalizability of our findings. It would have been interesting to examine the similarities or differences in rumination-related DMN – sgPFC connectivity between a rMDD group and an MDD group. Nevertheless, our results are consistent with prior fMRI studies concerning DMN hyper-connectivity and its association with maladaptive rumination.

Future research should expand on these findings by inducing participants into a ruminative state, in addition to the unconstrained resting state. Such a study would be able to determine whether elevated rumination-linked EEG PCC – sgPFC connectivity can be modulated by state factors, or if it is a stable electrophysiological trait. Future studies may also consider the use of non-invasive methods of brain stimulation. Transcranial Alternating Current Stimulation (tACS) is a promising technique to normalize frequency oscillations within regions of the brain. A recent brain stimulation study (Alexander et al., 2019) applied tACS on the left dorsolateral prefrontal cortex (DLPFC) of MDD patients to normalize elevated alpha power in an attempt to reduce depression symptoms. The tACS treatment protocol reduced left DLPFC alpha power, which resulted in lower depression symptoms. It would be important to evaluate whether tACS could normalize the elevated connectivity between DMN regions and the sgPFC, and whether such changes in connectivity would result in reduced maladaptive rumination.

In conclusion, our study found that EEG PCC – sgPFC functional connectivity was elevated within a group at-risk for depression. Moreover, we found that elevated connectivity between these regions was associated with rumination. This association was independent of current depression- and anxiety scores, suggesting that EEG PCC – sgPFC hyperconnectivity is a potential candidate biomarker of MDD risk.

Declaration of Competing Interest

Acknowledgments

Funding

References

Alexander, M.L., Alagapan, S., Lugo, C.E., Mellin, J.M., Lustenberger, C., Rubinow, D.R., Frohlich, F., 2019. Double-blind, randomized pilot clinical trial targeting alpha oscillations with transcranial alternating current stimulation (tACS) for the treatment of major depressive disorder (MDD). Transl. Psychiatry 9, 106.

Anand, A., Li, Y., Wang, Y., Wu, J., Gao, S., Bukhari, L., Mathews, V.P., Kalnin, A., Lowe, M.J., 2005. Activity and connectivity of brain mood regulating circuit in depression: a functional magnetic resonance study. Biol. Psychiatry 57, 1079–1088.

Andrews-Hanna, J.R., Reidler, J.S., Sepulcre, J., Poulin, R., Buckner, R.L., 2010. Functional-anatomic fractionation of the brain's default network. Neuron 65, 550–562.

Baillet, S., Mosher, J.C., Leahy, R.M., 2001. Electromagnetic brain mapping. IEEE Signal Proc. Mag. 18, 14–30.

Beck, A.T., Steer, R.A., Ball, R., Ranieri, W., 1996. Comparison of beck depression inventories -IA and -II in psychiatric outpatients. J. Pers. Assess. 67, 588–597.

Berman, M.G., Misic, B., Buschkuehl, M., Kross, E., Deldin, P.J., Peltier, S., Churchill, N. W., Jaeggi, S.M., Vakorin, V., McIntosh, A.R., Jonides, J., 2014. Does resting-state connectivity reflect depressive rumination? a tale of two analyses. Neuroimage 103, 267–279.

Berman, M.G., Peltier, S., Nee, D.E., Kross, E., Deldin, P.J., Jonides, J., 2011. Depression, rumination and the default network. Soc. Cogn. Affect. Neurosci. 6, 548–555.

Bigdely-Shamlo, N., Mullen, T., Kothe, C., Su, K.M., Robbins, K.A., 2015. The PREP pipeline: standardized preprocessing for large-scale EEG analysis. Front. Neuroinform. 9, 16.

Blackburn, I.M., Eunson, K.M., Bishop, S., 1986. A two-year naturalistic follow-up of depressed patients treated with cognitive therapy, pharmacotherapy and a combination of both. J. Affect. Disord. 10, 67–75.

Brookes, M.J., Hale, J.R., Zumer, J.M., Stevenson, C.M., Francis, S.T., Barnes, G.R., Owen, J.P., Morris, P.G., Nagarajan, S.S., 2011. Measuring functional connectivity using MEG: methodology and comparison with fcMRI. Neuroimage 56, 1082–1104.

Brookes, M.J., Woolrich, M.W., Barnes, G.R., 2012. Measuring functional connectivity in MEG: a multivariate approach insensitive to linear source leakage. Neuroimage 63, 910–920.

Buckner, R.L., Andrews-Hanna, J.R., Schacter, D.L., 2008. The brain's default network: anatomy, function, and relevance to disease. Ann. N. Y. Acad. Sci. 1124, 1–38.

Chang, C.Y., Hsu, S.H., Pion-Tonachini, L., Jung, T.P., 2020. Evaluation of artifact subspace reconstruction for automatic artifact components removal in multi-channel EEG recordings. IEEE Trans. Biomed. Eng. 67, 1114–1121.

Chen, A.C., Oathes, D.J., Chang, C., Bradley, T., Zhou, Z.W., Williams, L.M., Glover, G.H., Deisseroth, K., Etkin, A., 2013. Causal interactions between fronto-parietal central executive and default-mode networks in humans. Proc. Natl. Acad. Sci. U. S. A. 110, 19944–19949.

Colclough, G.L., Woolrich, M.W., Tewarie, P.K., Brookes, M.J., Quinn, A.J., Smith, S.M., 2016. How reliable are MEG resting-state connectivity metrics? Neuroimage 138, 284–293.

Damoiseaux, J.S., Beckmann, C.F., Arigita, E.J., Barkhof, F., Scheltens, P., Stam, C.J., Smith, S.M., Rombouts, S.A., 2008. Reduced resting-state brain activity in the "default network" in normal aging. Cereb. Cortex 18, 1856–1864.

Delorme, A., Makeig, S., 2004. EEGLAB: an open source toolbox for analysis of single-trial EEG dynamics including independent component analysis. J. Neurosci. Methods 134, 9–21.

Eaton, W.W., Shao, H., Nestadt, G., Lee, H.B., Bienvenu, O.J., Zandi, P., 2008. Population-based study of first onset and chronicity in major depressive disorder. Arch. Gen. Psychiatry 65, 513–520.

Etkin, A., Egner, T., Kalisch, R., 2011. Emotional processing in anterior cingulate and medial prefrontal cortex. Trends Cogn. Sci. 15, 85–93.

Fingelkurts, A.A., Fingelkurts, A.A., 2015. Altered structure of dynamic electroencephalogram oscillatory pattern in major depression. Biol. Psychiatry 77, 1050–1060.

First, M., Spitzer, R.L., Gibbon, M.L., Williams, J., 2002. Structured clinical interview for DSM-IV-TR Axis I Disorders, Research Version, Non-patient Edition.

Flett, G.L., Madorsky, D., Hewitt, P.L., Heisel, M.J., 2002. Perfectionism cognitions, rumination, and psychological distress. J. Rational-Emot. Cognit. Behav. Therapy 20, 33–47.

Friedrich, M.J., 2017. Depression is the leading cause of disability around the world. JAMA 317, 1517.

Gaffrey, M.S., Luby, J.L., Botteron, K., Repovs, G., Barch, D.M., 2012. Default mode network connectivity in children with a history of preschool onset depression. J. Child Psychol. Psychiatry 53, 964–972.

Glasser, M.F., Sotiropoulos, S.N., Wilson, J.A., Coalson, T.S., Fischl, B., Andersson, J.L., Xu, J., Jbabdi, S., Webster, M., Polimeni, J.R., Van Essen, D.C., Jenkinson, M., Consortium, W.U.-M.H., 2013. The minimal preprocessing pipelines for the Human Connectome Project. Neuroimage 80, 105–124.

Gramfort, A., Papadopoulo, T., Olivi, E., Clerc, M., 2010. OpenMEEG: opensource software for quasistatic bioelectromagnetics. Biomed. Eng. Online 9, 45.

Greicius, M.D., Flores, B.H., Menon, V., Glover, G.H., Solvason, H.B., Kenna, H., Reiss, A. L., Schatzberg, A.F., 2007. Resting-state functional connectivity in major depression: abnormally increased contributions from subgenual cingulate cortex and thalamus. Biol. Psychiatry 62, 429–437.

Guo, W., Liu, F., Dai, Y., Jiang, M., Zhang, J., Yu, L., Long, L., Chen, H., Gao, Q., Xiao, C., 2013. Decreased interhemispheric resting-state functional connectivity in first-episode, drug-naive major depressive disorder. Prog. Neuropsychopharmacol. Biol. Psychiatry 41, 24–29.

Guo, W., Liu, F., Zhang, J., Zhang, Z., Yu, L., Liu, J., Chen, H., Xiao, C., 2014. Abnormal default-mode network homogeneity in first-episode, drug-naive major depressive disorder. PLoS ONE 9, e91102.

Gusnard, D.A., Akbudak, E., Shulman, G.L., Raichle, M.E., 2001. Medial prefrontal cortex and self-referential mental activity: relation to a default mode of brain function. Proc. Natl. Acad. Sci. U. S. A. 98, 4259–4264.

Hamilton, J.P., Chen, G., Thomason, M.E., Schwartz, M.E., Gotlib, I.H., 2011a. Investigating neural primacy in Major Depressive Disorder: multivariate Granger causality analysis of resting-state fMRI time-series data. Mol. Psychiatry 16, 763–772.

Hamilton, J.P., Farmer, M., Fogelman, P., Gotlib, I.H., 2015. Depressive rumination, the default-mode network, and the dark matter of clinical neuroscience. Biol. Psychiatry 78, 224–230.

Hamilton, J.P., Furman, D.J., Chang, C., Thomason, M.E., Dennis, E., Gotlib, I.H., 2011b. Default-mode and task-positive network activity in major depressive disorder: implications for adaptive and maladaptive rumination. Biol. Psychiatry 70, 327–333.

Hlinka, J., Alexakis, C., Diukova, A., Liddle, P.F., Auer, D.P., 2010. Slow EEG pattern predicts reduced intrinsic functional connectivity in the default mode network: an inter-subject analysis. Neuroimage 53, 239–246.

Ho, T.C., Connolly, C.G., Henje Blom, E., LeWinn, K.Z., Strigo, I.A., Paulus, M.P., Frank, G., Max, J.E., Wu, J., Chan, M., Tapert, S.F., Simmons, A.N., Yang, T.T., 2015. Emotion-dependent functional connectivity of the default mode network in adolescent depression. Biol. Psychiatry 78, 635–646.

Ito, T., Takenaka, K., Agari, I., 2005. Psychological vulnerability to depression: negative rumination, perfectionism, immodithymic personality, dysfunctional attitudes, and depressive states. Jpn. J. Educ. Psychol. 53, 162–171.

Joormann, J., Dkane, M., Gotlib, I.H., 2006. Adaptive and maladaptive components of rumination? diagnostic specificity and relation to depressive biases. Behav. Ther. 37, 269–280.

Joshi, A., Choi, S., Sonkar, G., Chong, M., Gonzalez-Martinez, J., Nair, D., Shattuck, D., Damasio, H., Leahy, R., 2017. A Whole Brain Atlas With Sub-Parcellation of Cortical Gyri Using Resting fMRI.

Kato, M., Hori, H., Inoue, T., Iga, J., Iwata, M., Inagaki, T., Shinohara, K., Imai, H., Murata, A., Mishima, K., Tajika, A., 2020. Discontinuation of antidepressants after remission with antidepressant medication in major depressive disorder: a systematic review and meta-analysis. Mol. Psychiatry.

Kruijshaar, M.E., Barendregt, J., Vos, T., de Graaf, R., Spijker, J., Andrews, G., 2005. Lifetime prevalence estimates of major depression: an indirect estimation method and a quantification of recall bias. Eur. J. Epidemiol. 20, 103–111.

Lei, X., Wang, Y., Yuan, H., Mantini, D., 2014. Neuronal oscillations and functional interactions between resting state networks. Hum. Brain Mapp. 35, 3517–3528.

Lei, X., Zhao, Z., Chen, H., 2013. Extraversion is encoded by scale-free dynamics of default mode network. Neuroimage 74, 52–57.

Li, B., Liu, L., Friston, K.J., Shen, H., Wang, L., Zeng, L.L., Hu, D., 2013. A treatment-resistant default mode subnetwork in major depression. Biol. Psychiatry 74, 48–54.

Li, B.J., Friston, K., Mody, M., Wang, H.N., Lu, H.B., Hu, D.W., 2018. A brain network model for depression: from symptom understanding to disease intervention. CNS Neurosci. Ther. 24, 1004–1019.

Lyubomirsky, S., Nolen-Hoeksema, S., 1993. Self-perpetuating properties of dysphoric rumination. J. Pers. Soc. Psychol. 65, 339–349.

Makeig, S., Bell, A.J., Jung, T.-P., Sejnowski, T.J., 1995. Independent component analysis of electroencephalographic data. In: Proceedings of the 8th International Conference on Neural Information Processing Systems. MIT Press, Denver, Colorado, pp. 145–151.

Mantini, D., Perrucci, M.G., Del Gratta, C., Romani, G.L., Corbetta, M., 2007. Electrophysiological signatures of resting state networks in the human brain. Proc. Natl. Acad. Sci. U. S. A. 104, 13170–13175.

Marroquín, B.M., Fontes, M., Scilletta, A., Miranda, R., 2010. Ruminative subtypes and coping responses: active and passive pathways to depressive symptoms. Cognit. Emotion 24, 1446–1455.

Michel, C., He, B., 2012. EEG mapping and source imaging. Niedermeyer's Electroencephalography 1179–1202.

Neuner, I., Arrubla, J., Werner, C.J., Hitz, K., Boers, F., Kawohl, W., Shah, N.J., 2014. The default mode network and EEG regional spectral power: a simultaneous fMRI-EEG study. PLoS ONE 9, e88214.

Ney, J.P., van der Goes, D.N., Nuwer, M.R., Nelson, L., Eccher, M.A., 2013. Continuous and routine EEG in intensive care: utilization and outcomes, United States 2005-2009. Neurology 81, 2002–2008.

Nixon, N.L., Liddle, P.F., Nixon, E., Worwood, G., Liotti, M., Palaniyappan, L., 2014. Biological vulnerability to depression: linked structural and functional brain network findings. Br. J. Psychiatry 204, 283–289.

Nolan, S.A., Roberts, J.E., Gotlib, I.H., 1998. Neuroticism and ruminative response style as predictors of change in depressive symptomatology. Cognit. Ther. Res. 22, 445–455.

Nolen-Hoeksema, S., Morrow, J., 1991. A prospective study of depression and posttraumatic stress symptoms after a natural disaster: the 1989 Loma Prieta Earthquake. J. Pers. Soc. Psychol. 61, 115–121.

Nolen-Hoeksema, S., Parker, L.E., Larson, J., 1994. Ruminative coping with depressed mood following loss. J. Pers. Soc. Psychol. 67, 92–104.

Nolen-Hoeksema, S., Wisco, B.E., Lyubomirsky, S., 2008. Rethinking rumination. Perspect. Psychol. Sci. 3, 400–424.

Northoff, G., Bermpohl, F., 2004. Cortical midline structures and the self. Trends Cogn. Sci. 8, 102–107.

Olbrich, S., Arns, M., 2013. EEG biomarkers in major depressive disorder: discriminative power and prediction of treatment response. Int. Rev. Psychiatry 25, 604–618.

Olbrich, S., Tränkner, A., Chittka, T., Hegerl, U., Schönknecht, P., 2014. Functional connectivity in major depression: increased phase synchronization between frontal cortical EEG-source estimates. Psychiatry Res. 222, 91–99.

Perrin, F., Pernier, J., Bertrand, O., Giard, M.H., Echallier, J.F., 1987. Mapping of scalp potentials by surface spline interpolation. Electroencephalogr. Clin. Neurophysiol. 66, 75–81.

Raichle, M.E., MacLeod, A.M., Snyder, A.Z., Powers, W.J., Gusnard, D.A., Shulman, G.L., 2001. A default mode of brain function. Proc. Natl. Acad. Sci. USA 98, 676–682.

Sestieri, C., Corbetta, M., Romani, G.L., Shulman, G.L., 2011. Episodic memory retrieval, parietal cortex, and the default mode network: functional and topographic analyses. J. Neurosci. 31, 4407–4420.

Sheline, Y.I., Price, J.L., Yan, Z., Mintun, M.A., 2010. Resting-state functional MRI in depression unmasks increased connectivity between networks via the dorsal nexus. Proc. Natl. Acad. Sci. U. S. A. 107, 11020–11025.

Song, J., Davey, C., Poulsen, C., Luu, P., Turovets, S., Anderson, E., Li, K., Tucker, D., 2015. EEG source localization: sensor density and head surface coverage. J. Neurosci. Methods 256, 9–21.

Spasojević, J., Alloy, L.B., 2001. Rumination as a common mechanism relating depressive risk factors to depression. Emotion 1, 25–37.

Spreng, R.N., Mar, R.A., Kim, A.S., 2009. The common neural basis of autobiographical memory, prospection, navigation, theory of mind, and the default mode: a quantitative meta-analysis. J. Cogn. Neurosci. 21, 489–510.

Tadel, F., Baillet, S., Mosher, J.C., Pantazis, D., Leahy, R.M., 2011. Brainstorm: a user-friendly application for MEG/EEG analysis. Comput. Intell. Neurosci. 2011, 879716.

Takano, K., Tanno, Y., 2009. Self-rumination, self-reflection, and depression: self-rumination counteracts the adaptive effect of self-reflection. Behav. Res. Ther. 47, 260–264.

Treynor, W., Gonzalez, R., Nolen-Hoeksema, S., 2003. Rumination reconsidered: a psychometric analysis. Cognit. Ther. Res. 27, 247–259.

Vanderhasselt, M.A., De Raedt, R., Dillon, D.G., Dutra, S.J., Brooks, N., Pizzagalli, D.A., 2012. Decreased cognitive control in response to negative information in patients with remitted depression: an event-related potential study. J. Psychiatry Neurosci. 37, 250–258.

Vorwerk, J., Cho, J.H., Rampp, S., Hamer, H., Knosche, T.R., Wolters, C.H., 2014. A guideline for head volume conductor modeling in EEG and MEG. Neuroimage 100, 590–607.

Watson, D., Clark, L., Weber, K., Assenheimer, J., Strauss, M., McCormick, R., 1995. Testing a tripartite model: ii. exploring the symptom structure of anxiety and depression in student, adult, and patient samples. J. Abnorm. Psychol. 104, 15–25.

Whitton, A.E., Deccy, S., Ironside, M.L., Kumar, P., Beltzer, M., Pizzagalli, D.A., 2018. Electroencephalography source functional connectivity reveals abnormal high-frequency communication among large-scale functional networks in depression. Biol. Psychiatry Cogn. Neurosci. Neuroimaging 3, 50–58.

World Health Organization, W., 2017. Depression and Other Common Mental disorders: Global Health Estimates. World Health Organization, Geneva.

Xu, X., Yuan, H., Lei, X., 2016. Activation and connectivity within the default mode network contribute independently to future-oriented thought. Sci. Rep. 6, 21001.

Yekutieli, D., Benjamini, Y., 1999. Resampling-based false discovery rate controlling multiple test procedures for correlated test statistics. J. Stat. Plan. Inference 82, 171–196.

Zamoscik, V., Huffziger, S., Ebner-Priemer, U., Kuehner, C., Kirsch, P., 2014. Increased involvement of the parahippocampal gyri in a sad mood predicts future depressive symptoms. Soc. Cogn. Affect. Neurosci. 9, 2034–2040.

Zhou, H.X., Chen, X., Shen, Y.Q., Li, L., Chen, N.X., Zhu, Z.C., Castellanos, F.X., Yan, C.G., 2020. Rumination and the default mode network: meta-analysis of brain imaging studies and implications for depression. Neuroimage 206, 116287.

Zhu, X., Wang, X., Xiao, J., Liao, J., Zhong, M., Wang, W., Yao, S., 2012. Evidence of a dissociation pattern in resting-state default mode network connectivity in first-episode, treatment-naive major depression patients. Biol. Psychiatry 71, 611–617.